

Article

Low Loss Sol-Gel TiO₂ Thin Films for Waveguiding Applications

Tahar Touam¹, Lamia Znaidi^{2,*}, Dominique Vrel², Iva Ninova-Kuznetsova², Ovidiu Brinza², Alexis Fischer³ and Azzedine Boudrioua³

¹ Laboratory of Semiconductors, University of Badji Mokhtar, BP 12, Annaba 23000, Algeria; E-Mail: touamt@gmail.com

² Laboratory of Sciences of Processes and Materials (LSPM), CNRS-UPR 3407, Paris 13 University, Sorbonne Paris Cité, 99-Jean-Baptiste Clément Avenue, Villetaneuse 93430, France; E-Mails: dominique.vrel@lspm.cnrs.fr (D.V.); ninovai@yahoo.com (I.N.-K.); ovidiu.brinza@lspm.cnrs.fr (O.B.)

³ Lasers Physics Laboratory (LPL), CNRS-UMR 7538, Paris 13 University, Sorbonne Paris Cité, 99-Jean-Baptiste Clément Avenue, Villetaneuse 93430, France; E-Mails: fischer@iutv.univ-paris13.fr (A.F.); boudrioua@univ-paris13.fr (A.B.)

* Author to whom correspondence should be addressed; E-Mail: lamia.znaidi@lspm.cnrs.fr; Tel.: +33-1-49-40-34-45; Fax: +33-1-49-40-34-14.

Received: 21 January 2013; in revised form: 27 February 2013 / Accepted: 1 March 2013 / Published: 11 March 2013

Abstract: TiO₂ thin films were synthesized by sol-gel process: titanium tetraisopropoxide (TTIP) was dissolved in isopropanol, and then hydrolyzed by adding a water/isopropanol mixture with a controlled hydrolysis ratio. The as prepared sol was deposited by “dip-coating” on a glass substrate with a controlled withdrawal speed. The obtained films were annealed at 350 and 500 °C (2 h). The morphological properties of the prepared films were analyzed by Scanning Electron Microscopy (SEM) and Atomic Force Microscopy (AFM). The optical waveguiding properties of TiO₂ films were investigated for both annealing temperature using m-lines spectroscopy. The refractive indices and the film thickness were determined from the measured effective indices. The results show that the synthesized planar waveguides are multimodes and demonstrate low propagation losses of 0.5 and 0.8 dB/cm for annealing temperature 350 and 500 °C, respectively.

Keywords: sol-gel; TiO₂ thin films; optical properties; waveguides; propagation losses

1. Introduction

Titanium dioxide (TiO_2) is attracting a considerable amount of research interest due to its interesting chemical, electrical and optical properties. TiO_2 has a large refractive index among the transparent metal oxides (>2.5 at anatase phase, and >2.7 at rutile phase). The optical absorption loss of TiO_2 is about 10 times lower than silicon at optical communication wavelength of 1.55 μm [1]. Its thermal expansion coefficient is very small over a wide range from room temperature to 1000 $^\circ\text{C}$, and it is transparent over a wide range of wavelength. Considering all of these advantages, TiO_2 has been considered for various optical applications such as high refractive index component of multilayer optical filter [2], sensors [3], antireflective coating [4,5], photocatalysts [6,7], integrated optical planar waveguides and devices [8,9], solar cell [10], IR detectors [11], optoelectronics and photovoltaics [12,13], optical amplifiers [14], and micro-nano photonic crystal structures [15].

Metal oxides thin films have been made by a variety of methods. One of these, the sol-gel process [16–18], reflects distinct advantages due to its excellent compositional control, homogeneity on the molecular level, simplicity, low cost, performing well in atmospheric pressure without the need for expensive vacuum equipment, lower crystallization temperature, possibility to easily incorporate rare-earth ions as optically active centers and it can be used to deposit films over a large area with a very uniform thickness. It allows the tuning of the refractive index and thickness of the film by varying synthesis parameters.

Several studies have been reported on TiO_2 thin films elaboration by sol-gel process [19–21] and indicated that their structural and optical properties depend on the synthesis parameters used in the process.

In this paper, we report the study of the morphological, optical and waveguiding properties of TiO_2 thin films deposited on glass substrates by sol-gel process. To previously obtained results [22], additional experiments have been performed to prove the reproducibility of optical measurements and additional morphological characterizations are here presented.

2. Experimental Section

TiO_2 thin films were prepared by the sol-gel process according to the following procedure: titanium tetraisopropoxide (TTIP) diluted in isopropanol was hydrolyzed by a water/isopropanol mixture with a controlled hydrolysis ratio ($h = [\text{H}_2\text{O}]/[\text{TTIP}] = 1.4$) and for 1 molar final titanium concentration. Glass substrates were dipped in the freshly prepared sol and then withdrawn at a constant withdrawal speed of 2 cm min^{-1} (“dip-coating”). Four layers were deposited for increasing the thickness after solvent evaporation, at 80 $^\circ\text{C}$, between two coatings. The obtained films were annealed at 350 and 500 $^\circ\text{C}$ (2 h) and will be called, in this work, TiO_2 -350 and TiO_2 -500, respectively.

The characterizations by Scanning Electronic Microscopy (SEM) and Atomic Force Microscopy (AFM) were performed with a Leica S440 microscope and a Veeco Nanoscope DIM3. Optical characterization of the films has been carried out using m-lines spectroscopy [23]. The refractive indices and the film thickness were determined from the measured effective indices.

3. Results and Discussion

3.1. Morphological Characterizations

Figure 1 presents high-magnification SEM images of the same samples. The TiO₂-350 sample (Figure 1a) yielded a SEM observation depicting a perfectly smooth surface, using magnifications of up to 100,000. As for the TiO₂-500 sample (Figure 1b), it is homogeneous and seems to be constituted of small platelet particles, ranging from 30 to 100 nm in length, and from 10 to 20 nm in thickness, embedded in a continuous phase which may be a rest of amorphous phase. Indeed, from XRD measurements (Figure 2) [22], we concluded that at 350 °C the TiO₂ films are amorphous, but crystallize in anatase form when heated up to 500 °C.

Figure 1. SEM images of TiO₂ thin films: (a) TiO₂-350 and (b) TiO₂-500 samples (magnification $\times 50,000$).

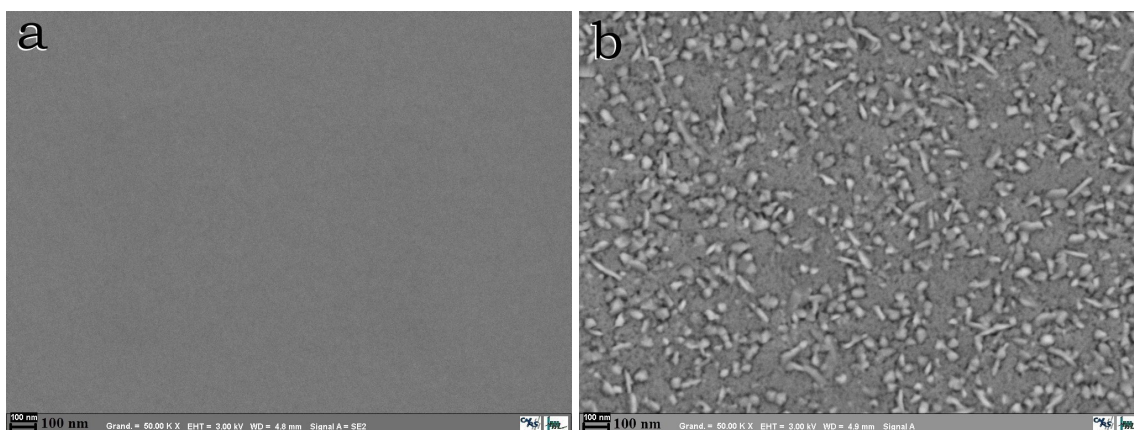
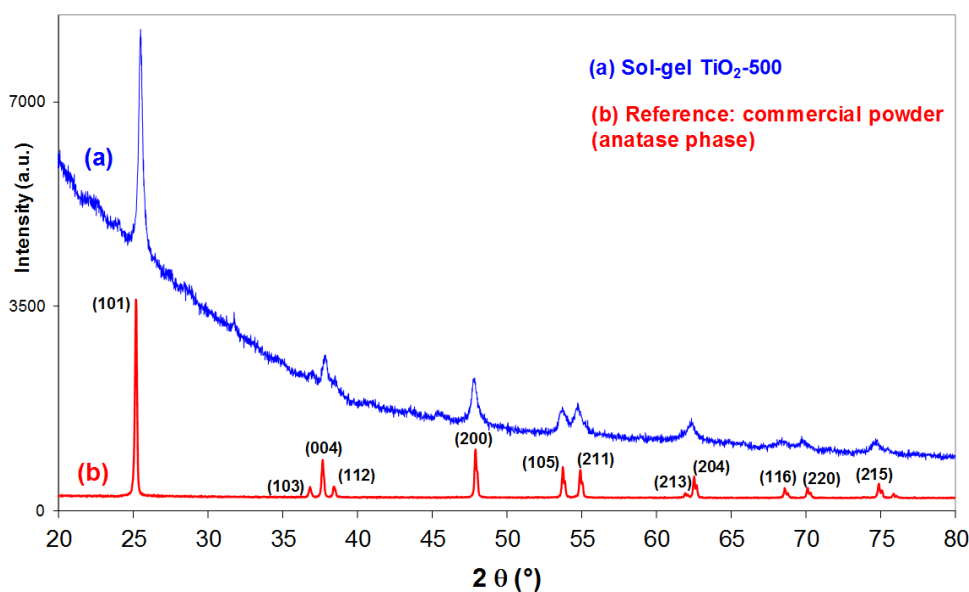


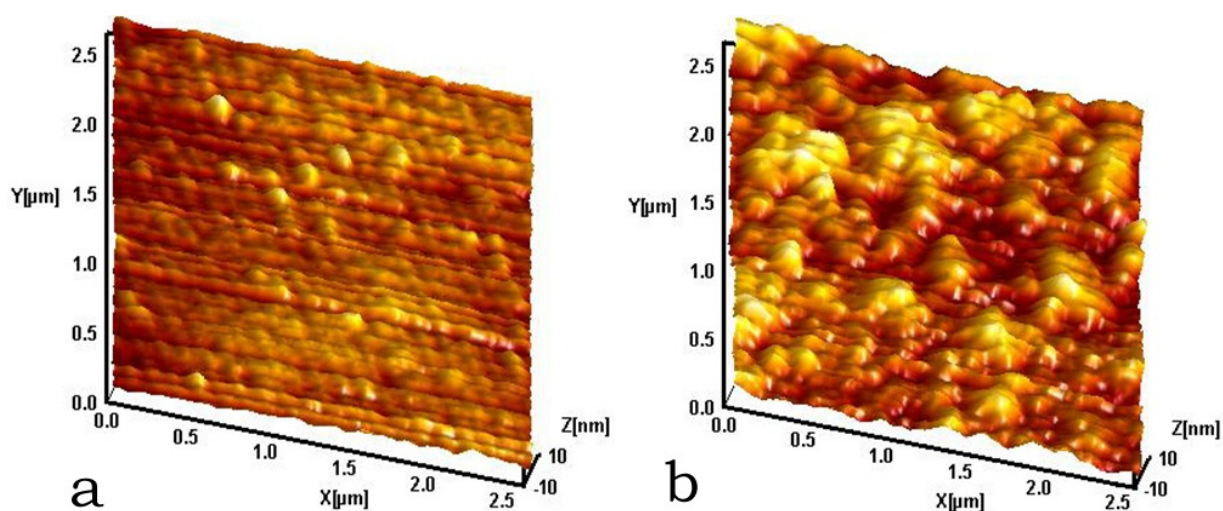
Figure 2. X-ray diffraction patterns of TiO₂-500 sample and commercial powder as a reference [22].



AFM images (Figure 3) show the surface morphologies of the both samples and from these images, the Roughness Mean Square (RMS) values were measured at 1.65 nm and 3.26 nm for TiO₂-350 and TiO₂-500 films, respectively. TiO₂-350 film has an extremely small roughness which is consistent with the smooth surface observed by SEM analysis. On the other hand, TiO₂-500 film shows a slightly greater roughness which is also consistent with its SEM image, showing two morphologies. Thus, the roughness seems to be dependent on the annealing temperature value. Our results and observations agree with the work of Mechiakh *et al.* [24] who reported that the RMS value was found to increase from 0.617 to 3.713 nm for sol-gel TiO₂ thin films annealed at 350 and 450 °C, respectively; and that the increase in the roughness is due to the increase in the grain size. Similarly, Urlacher *et al.* [25] found, in the case of sol-gel ZrO₂ waveguides, that the amorphous film exhibits a smoother surface than the crystallized one, and the RMS varies from 0.2 to 2.1 nm, when increasing temperature from 300 up to 600 °C. From their analysis, this result is mainly due to crystallite growth when increasing temperature.

Due to our small roughness values, we may predict low optical losses for the waveguiding properties of the films. These properties are studied hereunder.

Figure 3. AFM images of TiO₂ thin films: (a) TiO₂-350 and (b) TiO₂-500 samples.



3.2. Optical Characterizations

The waveguiding features of TiO₂ thin films are investigated by dark m-lines spectroscopy technique [23,26]. This well known method allows us to obtain the optogeometric parameters of waveguiding thin films, such as thickness and refractive index. A right angle rutile prism is mounted onto a precise rotary stage (0.001°), which can be turned by a feedback-controlled DC motor. The mode profiles in both the TE (transverse electric) and TM (transverse magnetic) polarizations are obtained by measuring the reflected intensity of a He-Ne laser beam operating at a 632.8 nm wavelength, as a function of the incidence angle. The corresponding effective mode indices can thus be calculated. Consequently, we can determine the refractive indices n_{TE} and n_{TM} for the TE and TM polarization, respectively, and the thickness of films. Figures 4 and 5 display typical TE and TM guided mode spectra of the TiO₂ films for two samples TiO₂-350 and TiO₂-500, respectively. We observe the excitation of two guided modes for TE and TM polarization for the TiO₂-350 sample and two guided modes for TE and only one guided mode for TM for the TiO₂-500 sample.

From the angular position of the reflectivity dips we compute the effective mode indices, which then serve to calculate the refractive indices and the thickness of the layer through the following dispersion relationship [23]:

$$\frac{2\pi d}{\lambda} (n^2 - N_m^2)^{1/2} = m\pi + \Phi_{(n,na)} + \Phi_{(n,ns)} \tag{1}$$

where:

$$\Phi_{(n,n_j)} = \arctan \left[\left(\frac{n}{n_j} \right)^{2\rho} \left(\frac{N_m^2 - n_j^2}{n^2 - N_m^2} \right) \right]^{1/2} \quad j = a, s \tag{2}$$

For TE mode $\rho = 0$ and $n = n_{TE}$ and for the TM mode $\rho = 1$ and $n = n_{TM}$; $\Phi_{(n,na)}$ and $\Phi_{(n,ns)}$ are the phase shift at air/film and film/substrate interfaces, d is the film thickness, λ is the wavelength of the light in vacuum, n_a and n_s are, respectively, the air and substrate refractive indices, m the mode number and N_m is the effective index of the m^{th} mode.

Figure 4. Typical guided mode spectra of TiO₂-350 thin film: (a) transverse electric (TE) and (b) transverse magnetic (TM) polarizations.

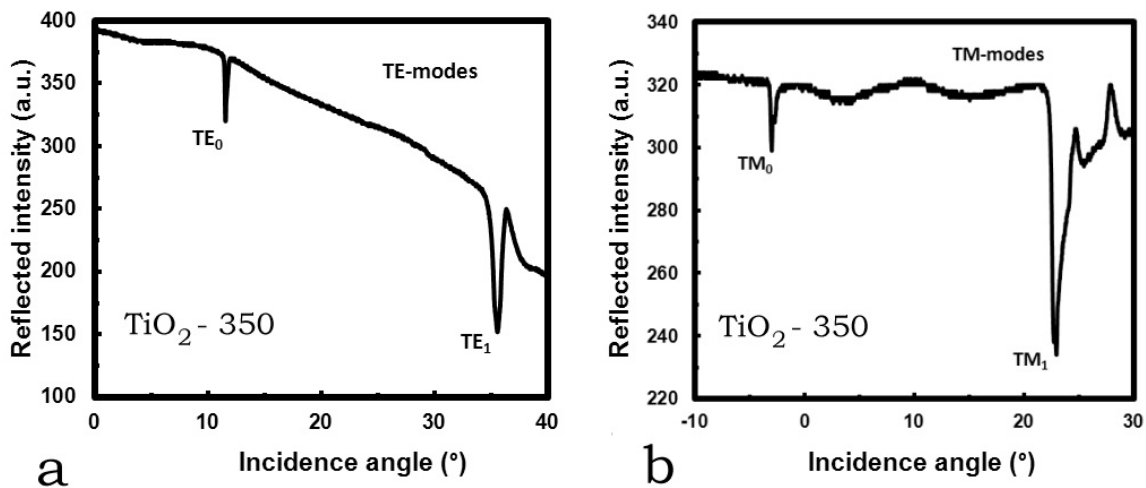
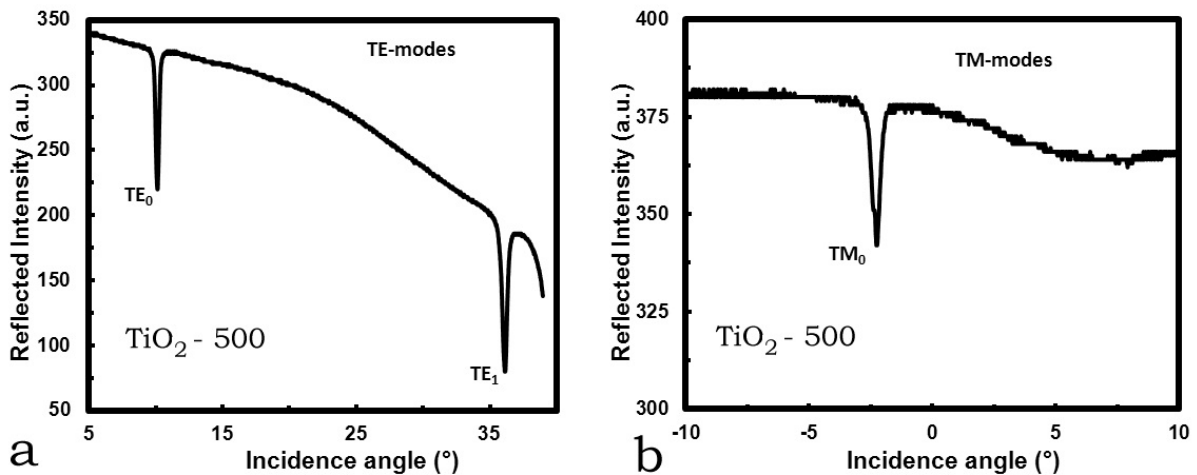


Figure 5. Typical guided mode spectra of TiO₂-500 thin film: (a) TE and (b) TM polarizations.



From the angular position of TE and TM guided modes (Figures 4 and 5) we deduced the corresponding effective indices. These values are then used to compute the thin film parameters: ordinary refractive index (n_{TE}), extraordinary refractive index (n_{TM}) and thickness (d). The calculation is based on the least square method widely discussed by Kersten [27]. In the case of Figure 4 ($T = 350$ °C), we found $n_{TE} = 1.9720$, $n_{TM} = 1.9895$ and $d = 358$ nm. While for the case of Figure 5 ($T = 500$ °C), we found $n_{TE} = 1.9949$, $n_{TM} = 2.0092$ and $d = 336$ nm. Finally, from the refractive index and thickness, we computed the theoretical effective indices of the thin films. The results are reported in Table 1. We notice a very good agreement between measured and calculated values of effective indices.

The results show that refractive index increases with annealing temperature while thickness decreases due to shrinkage and densification of the films. These results are in good agreement with the work of Wang *et al.* [28] who found, in the case of sol-gel TiO₂ waveguides, that the film thickness decreases and the refractive index increases when the heat treatment temperature increases. Urlacher *et al.* [25] reported, in the case of ZrO₂ film, that the thickness roughly decreases between 300 and 400 °C indicating a high densification of the layer before crystallization. Refractive index simultaneously increases as a consequence of densification, organic compound removal and structural change in the material.

Table 1. Measured (N_m exp.) and computed (N_m th.) effective mode indices; and films thicknesses deduced from these measurements.

Sample	Polarization	m	N_m exp.	N_m th.	ΔN_m	n	d (nm)
TiO ₂ -350	TE	0	1.8687	1.8685	2×10^{-4}	1.9720	358
	TE	1	1.5664	1.5659	5×10^{-4}		
	TM	0	1.8444	1.8442	2×10^{-4}	1.9895	
	TM	1	1.5135	1.5134	1×10^{-4}		
TiO ₂ -500	TE	0	1.8816	1.8814	2×10^{-4}	1.9949	336
	TE	1	1.5532	1.5527	5×10^{-4}		
	TM	0	1.8479	1.8475	4×10^{-4}	2.0092	

The sharpness of the reflectivity dips, observed on Figures 4 and 5, indicates a good optical confinement of the light beam into the thin films. Measurements of the losses will bring more insight about this point. Indeed, the determination of optical attenuation in waveguides is of great interest for designing integrated optical devices. Practical use of such structures directly depends on the measurement of this parameter. Several techniques have been used for loss measurement among which the end-fire coupling [29], the prism coupling method [30], and a new approach that uses a prism-in coupling method to feed the light into the waveguide and the end-fire coupling to measure the transmitted light [31].

For optical losses measurement, we used the prism-in coupling method (Metricon Model 2010) in which the exponential decay of light is measured by a fiber probe scanning down the length of the propagation streak. A least square exponential fit is then made to the intensity as a function of distance patterns and the loss is calculated in decibels per centimeter (dB/cm). The overall loss measured is the combined total of both scattering loss from particles or other scattering centers and surface roughness, and the inherent absorption of the waveguide material.

The results of the optical attenuation of the fundamental TE mode in TiO₂ thin films annealed at 350 and 500 °C are shown in Figure 6a,b. The optical losses have been estimated around $\alpha = 0.5$ dB/cm and $\alpha = 0.80$ dB/cm, respectively, using the following equation:

$$\alpha = -\frac{10}{L} \log\left(\frac{I_L}{I_0}\right) \quad (3)$$

where I_0 is the initial light intensity, and I_L is the light intensity at the considered position L , measured in centimeters.

Table 2 summarizes the structural and optical characteristics of both samples.

Figure 6. Optical attenuation of the fundamental TE mode in TiO₂ thin film (a) TiO₂-350 and (b) TiO₂-500 samples: surface scattering measurement (dotted line), with exponential fit (in red).

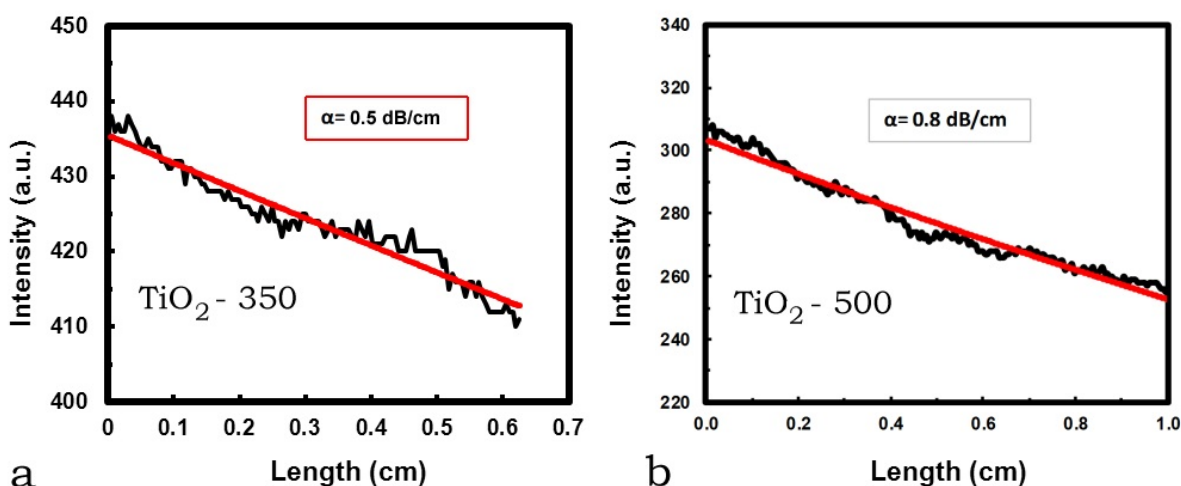


Table 2. Comparison of films characteristics. The refractive indices and attenuation values are given for the fundamental TE mode.

Sample	H.T.T (°C) *	Structure [22]	Thickness: d (nm)	RMS (nm)	Refractive index: n	Attenuation: α (dB/cm)
TiO ₂ -350	350	Amorphous	358	1.65	1.9720	0.5
TiO ₂ -500	500	Crystallized	336	3.26	1.9949	0.8

* H.T.T: heat treatment temperature.

As we reported above, TiO₂-350 sample is amorphous while TiO₂-500 is crystallized and the film thickness decreases with annealing temperature. From our results, we can deduce that increasing annealing temperature leads to increasing RMS, refractive index and optical losses. Similar results on the increase of optical losses with the annealing temperature were already reported on sol-gel ZrO₂ [25,32] and TiO₂ [33] films. For the former, Ehrhart *et al.* [32] reported that in order to obtain ZrO₂ thin films with a high refractive index ($n = 1.96$) and low optical losses (0.29 dB/cm), the best heat-treatment corresponds to an annealing at 400 °C, thus preserving an amorphous phase, while optical losses increase at a temperature of 450 °C when the crystallization into a metastable tetragonal phase appears; Urlacher *et al.* [25] also found that ZrO₂ optical losses increase when the annealing temperature

and film crystallinity increase: they obtained 0.8 and 2.5 dB/cm as attenuation coefficients for the amorphous film heat treated at 300 °C and the crystallized film annealed at 600 °C, respectively. For the latter, Bahtat *et al.* [33] reported that at lower temperatures (450 °C), the films' structure consists of a mixture of amorphous TiO₂ and anatase nanocrystals and its surface is smooth. On the contrary, when increasing the annealing temperature, crystallization increases yielding a higher roughness and the films' waveguiding properties disappear.

4. Conclusions

In this work we reported the investigation of TiO₂ thin films prepared by sol-gel process for optical waveguiding applications. The surface morphologies observed by SEM and AFM have shown that the quality of the films present a low roughness when the annealing temperature is 350 °C, but increases at an annealing temperature of 500 °C.

The optical properties were determined by m-lines spectroscopy. The synthesized thin films are displaying several guided modes meaning that the coupling and confinement of the light in the film is efficient. The results show that the refractive index increases with annealing temperature, due to a higher densification of the film. The optical losses of the amorphous film, annealed at 350 °C, and the crystallized one, annealed at 500 °C, were estimated to be around 0.5 and 0.8 dB/cm, respectively, from surface scattering measurement using the moving fiber method. This work emphasizes the importance of the film microstructure determination and clearly shows the correlation between structural and optical properties. The sol-gel process seems therefore very promising for the synthesis of planar waveguides for integrated photonics, especially when heat treated below the crystallization temperature. Moreover, we believe that by optimizing the synthesis parameters of the process, the optical losses can be decreased to less than 0.3 dB/cm.

Acknowledgments

ANR (Agence Nationale de la Recherche) and CGI (Commissariat à l'Investissement d'Avenir) are gratefully acknowledged for their financial support of this work through Labex SEAM (Science and Engineering for Advanced Materials and devices).

References

1. Yamasaki, S.; Hata, N.; Yoshida, T.; Oheda, H.; Matsuda, A.; Okushi, H.; Tanaka, K. Annealing studies on low optical absorption of GD a-Si:H using photoacoustic spectroscopy. *J. Phys. Colloq.* **1981**, *42*, C4-297–C4-300.
2. Brudnik, A.; Czternastek, H.; Zakrzewska, K.; Jachimowski, M. Plasma-emission-controlled d.c. magnetron sputtering of TiO_{2-x} thin films. *Thin Solid Films* **1991**, *199*, 45–58.
3. Garzella, C.; Comini, E.; Tempesti, E.; Frigeri, C.; Sberveglieri, G. TiO₂ thin films by a novel sol-gel processing for gas sensor applications. *Sens. Actuators B* **2000**, *68*, 189–196.
4. San Vicente, G.; Morales, A.; Gutiérrez, M.T. Sol-gel TiO₂ antireflective films for textured monocrystalline silicon solar cells. *Thin Solid Films* **2002**, *403–404*, 335–338.

5. Wongcharee, K.; Brungs, M.; Chaplin, R.; Hong, Y.J.; Pillar, R. Sol-gel processing by aging and pore creator addition for porous silica antireflective coatings. *J. Sol-Gel Sci. Technol.* **2002**, *25*, 215–221.
6. Yang, L.; Scott Saavedra, S.; Armstrong, N.R.; Hayes, J. Fabrication and characterization of low-loss, sol-gel planar waveguides. *Anal. Chem.* **1994**, *66*, 1254–1263.
7. Znaidi, L.; Seraphimova, R.; Bocquet, J.F.; Colbeau-Justin, C.; Pommier, C. A semi-continuous process for the synthesis of nanosize TiO₂ powders and their use as photocatalysts. *Mat. Res. Bull.* **2001**, *36*, 811–825.
8. Montagna, M.; Moser, E.; Visintainer, F.; Ferrari, M.; Zampedri, L.; Martucci, A.; Guglielmi, M.; Ivanda, M. Nucleation of titania nanocrystals in silica titania waveguides. *J. Sol-Gel Sci. Technol.* **2003**, *26*, 241–244.
9. Bernard, C.; Chaussement, S.; Monteil, A.; Ferrari, M. Molecular dynamics simulation of an Er-activated silica-titania glass: Composition influence on the structural properties. *Philos. Mag. B* **2002**, *82*, 681–693.
10. Yanagida, S.; Senadeera, G.K.R.; Nakamura, K.; Kitamura, T.; Wada, Y. Polythiophene-sensitized TiO₂ solar cells. *J. Photochem. Photobiol. A* **2004**, *166*, 75–80.
11. Shen, J.; Yang, T.; Zhang, Q.; Wang, J. Nanoporous TiO₂ coatings for infrared detectors. *J. Sol-Gel Sci. Technol.* **2003**, *26*, 1029–1032.
12. Wang, Z.; Helmersson, U.; Käll, P.O. Optical properties of anatase TiO₂ thin films prepared by aqueous sol-gel process at low temperature. *Thin Solid Films* **2002**, *405*, 50–54.
13. Pandiyan, R.; Micheli, V.; Ristic, D.; Bartali, R.; Pepponi, G.; Barozzi, M.; Gottardi, G.; Ferrari, M.; Laidani, N. Structural and near-infra red luminescence properties of Nd-doped TiO₂ films deposited by RF sputtering. *J. Mater. Chem.* **2012**, *22*, 22424–22432.
14. Conde-Gallardo, A.; García-Rocha, M.; Palomino-Merino, R.; Velásquez-Quesada, M.P.; Hernández-Calderón, I. Photoluminescence properties of Tb³⁺ and Eu³⁺ ions hosted in TiO₂ matrix. *Appl. Surf. Sci.* **2003**, *212–213*, 583–588.
15. Wang, X.; Fujimaki, M.; Awazu, K. Photonic crystal structures in titanium dioxide (TiO₂) and their optimal design. *Opt. Express* **2005**, *13*, 1486–1497.
16. Uhlmann, D.R.; Teowee, G. Sol-gel science and technology: Current state and future prospects. *J. Sol-Gel Sci. Technol.* **1998**, *13*, 153–162.
17. Hench, L.L.; West, J.K. The sol-gel process. *Chem. Rev.* **1990**, *90*, 33–72.
18. Znaidi, L. Sol-gel-deposited ZnO thin films: A review. *Mater. Sci. Eng. B* **2010**, *174*, 18–30.
19. Nishide, T.; Sato, M.; Hara, H. Crystal structure and optical property of TiO₂ gels and films prepared from Ti-edta complexes as titania precursors. *J. Mater. Sci.* **2000**, *35*, 465–469.
20. Oh, S.H.; Kim, D.J.; Hahn, S.H.; Kim, E.J. Comparison of optical and photocatalytic properties of TiO₂ thin films prepared by electron-beam evaporation and sol-gel dip-coating. *Mater. Lett.* **2003**, *57*, 4151–4155.
21. Znaidi, L.; Bocquet, J.F.; Pommier, C. Elaboration of TiO₂ nanometric powders and thin films aerogels. *AIDIC conf. Ser.* **2000**, *4*, 109–114.
22. Znaidi, L.; Touam, T.; Vrel, D.; Kuznetsova, I.N.; Fischer, A.; Boudrioua, A. Waveguiding properties of nanostructured TiO₂ thin films synthesized by sol-gel process. *AIP Conf. Proc.* **2011**, *1400*, 268–273.

23. Ulrich, R. Theory of the prism-film coupler by plane-wave analysis. *J. Opt. Soc. Am.* **1970**, *60*, 1337–1350.
24. Mechiakh, R.; Ben Sedrine, N.; Ben Naceur, J.; Chtourou, R. Elaboration and characterization of nanocrystalline TiO₂ thin films prepared by sol-gel dip-coating. *Surf. Coat. Technol.* **2011**, *206*, 243–249.
25. Urlacher, C.; Dumas, J.; Serughetti, J.; Mugnier, J.; Munoz, M. Planar ZrO₂ waveguides prepared by the sol-gel process: Structural and optical properties. *J. Sol-Gel Sci. Technol.* **1997**, *8*, 999–1005.
26. Tien, P.K.; Ulrich, R. Theory of prism-film coupler and thin-film light guides. *J. Opt. Soc. Am.* **1970**, *60*, 1325–1337.
27. Kersten, R.Th. Numerical solution of the mode-equation of planar dielectric waveguides to determine their refractive index and thickness by means of a prism-film coupler. *Opt. Commun.* **1973**, *9*, 427–431.
28. Wang, B.; Hu, L. Optical and surface properties of hybrid TiO₂/ormosil planar waveguide prepared by the sol-gel process. *Ceram. Int.* **2006**, *32*, 7–12.
29. Strohkendl, F.P.; Fluck, D.; Günter, P.; Irmscher, R.; Buchal, Ch. Nonleaky optical waveguides in KNbO₃ by ultralow dose MeV He ion implantation. *Appl. Phys. Lett.* **1991**, *59*, 3354–3356.
30. Weber, H.P.; Dunn, F.A.; Leibolt, W.N. Loss measurements in thin-film optical waveguides. *Appl. Opt.* **1973**, *12*, 755–757.
31. Boudrioua, A.; Loulergue, J.C. New approach for loss measurements in optical planar waveguides. *Opt. Commun.* **1997**, *137*, 37–40.
32. Ehrhart, G.; Capoen, B.; Robbe, O.; Boy, Ph.; Turrell, S.; Bouazaoui, M. Structural and optical properties of *n*-propoxide sol-gel derived ZrO₂ thin films. *Thin Solid Films* **2006**, *496*, 227–233.
33. Bahtat, M.; Mugnier, J.; Lou, L.; Serughetti, J. Planar TiO₂ waveguides by the sol-gel process: The relationship of structure to properties. *SPIE Proc.* **1992**, *1758*, 173.

© 2013 by the authors; licensee MDPI, Basel, Switzerland. This article is an open access article distributed under the terms and conditions of the Creative Commons Attribution license (<http://creativecommons.org/licenses/by/3.0/>).